Journal of Ovonic Research Vol. 8, No. 3, May - June 2012, p. 65 - 72

LIGHT EMITTING GERMANIUM AND SILICON NANOISLANDS GROWN BY RF MAGNETRON SPUTTERING

ALIREZA SAMAVATI[a*], FATIMA ALDAW[b], SIB KRISHNA GHOSHAL[c], ZULKAFLI OTHAMAN[a], SAMSUDI SAKRANI[b]
[a]*Ibn Sina Institute for Fundamental Science Studies, Universiti Teknologi Malaysia, 81310 Skudai, Johor Baharu, Malaysia*
[b]*Advanced Optical Material Research Group, Department of Physics, Faculty of Science, Universiti Teknologi Malaysia, 81310 UTM Skudai, Johor, Malaysia*
[c]*Department of Physics, Faculty of Science, Universiti Teknologi Malaysia, 81310 UTM Skudai, Johor, Malaysia*

The role of annealing temperature on the structural and optical properties of Ge and Si nanoislands deposited on Si(100) grown by radio frequency magnetron sputtering technique are studied. Atomic force microscopy confirmed the formation of Si and Ge nanoislands with estimated sizes lower than 100 nm and 45 nm respectively. The room temperature photoluminescence spectra for Si revealed an emission peak at 2.53 eV which is attributed to the formation of Si nanoislands whereas the observed strong luminescence peak at 3.22 eV for Ge nanoislands is attributed to the quantum size effect. A shift in the PL peak is observed upon annealing which is due to effect of quantum confinement and surface passivation by oxygen. The thermal annealing at 600 ^{0}C is found to play an important role in controlling the shape, number density, root mean square roughness and the energy shift of the luminescence band for both Si and Ge nanoislands. The influence of annealing on growth morphology for Ge nanoislands is appeared to be stronger than Si. The growth mechanism and the luminescence is analyzed and compared with other observations.

(Received March 5, 2012; Accepted May 2, 2012)

Keywords: Nanoislands; Optical Properties; Photoluminescence; Atomic Force Microscopy

1. Introduction

Nanostructuring of semiconductors is a novel means of developing new electronic and optoelectronic devices. In particular, the discovery of room-temperature visible photoluminescence (PL) from Si and Ge nanostructures has stimulated much interest in these particular kinds of nanoclusters and in small semiconductor particles [1-4]. The possibility of tuning the optical response of Si and Ge nanomaterials by modifying their size has become one of the most challenging aspects of recent semiconductor research. It has been established that quantum confinement (QC) can modify the energy gap that results visible luminescence as experimentally observed. Despite of numerous proposed models, experiments and simulations to explain the luminescence, including QC, surface states, defects in the oxides, core-shell structures and chemical complexes, however, the mechanism of visible PL is far from being understood. Over the past two decades the nanaostructure based devices has gradually been improved due to microelectronics and optoelectronics capabilities [5-9].

[*] Corresponding authors: alireza.samavati@yahoo.com

The economic fabrication of self-assembled Ge and Si nanostructure by radio frequency sputtering technique has received much attention for large-scale production. The synthesis of Ge nanostructures on Si substrate via Stranski-Krastanov growth mode has possibility to use for novel optical devices [6]. It is demonstrated that both Ge and Si upon nanosizing exhibits direct band gap and emit light in the visible region [7-11]. The magnetron sputtering method due to its high deposition rate and safety currently become one of the most popular commercially viable methods for fabricating the heterostructures of Ge\Si [12, 13] and Si\Si [11]. The luminescence from Ge and GeO_2 nanocrystals is observed around 3.1 eV and the strongest PL intensity evidenced for larger nanocrystals [14]. The PL spectra of Ge nanostructure having sizes between 2 and 9 nm can be viewed as a combination of three peaks at around 1.9, 2.3 and 3.0 eV as reported by Kartopu et al [15]. The Ge islands with height ~ 1 to 2 nm and widths ~ 40 to 50 nm are fabricated by Thanh et al in which the observed broadening in the PL spectra are explained in terms of the broad dispersion in the nanostructure size distribution [16]. Interestingly, the thermal annealing is found to influence strongly the structural and optical properties and produce a band gap energy shift ~ 0.25 eV as illustrated by Khan et al [17]. Zaho et al has reported the occurrence of the PL peak for Si nanoparticles at 1.65 eV [18]. Oku et al have demonstrated three prominent PL peaks for Si nanocrystals at 2.64, 2.52 and 2.25 eV and a peak for Ge at ~ 3.0 eV. The occurrence of these luminescence peaks is attributed to the formation of Si/SiO_x interface and quantum size effect of Si nanoclusters. In addition, the observed blue shift of the band gap energy is however attributed to the formation of the core-shell structure of Ge and Si with oxide layers [19].

Only few studies using sputtering method focused on the effect of annealing temperature dependent growth morphology and optical behavior of Ge and Si nanodots and the understanding on the mechanism of growth and luminescence is still lacking. Furthermore, careful fabrication and optical characterizations of such nanostructure is essential for controlled light emitting behavior that may be detrimental for optoelectronic devices. This research is targeted to provide some insight on the temperature dependent growth morphology by providing an efficient and easy fabrication method using RF sputtering. The results on structural and optical characterizations are presented, analyzed and the mechanism of annealing temperature dependent PL is understood.

2. Experimental details

The Ge and Si islands are separately sputtered on Si(100) substrate using high vacuum coater (HVC Penta Vacuum) .The samples are first cleaned ultrasonically in chromatic acid solution for 20 mins and then put in the chamber in order to remove the oxide and water vapor contaminations on the surface of Si substrate. Before the inlet of the argon gas the sputtering chamber is first evacuated down to 2.5×10^{-5} Torr. The growth process is carried out under conditions of fixed argon flow rate 10 Sccm, substrate temperatures 400°C, radio frequency power 100 W, chamber pressure 6×10^{-3} Torr, and deposition time of 300 sec. The rapid thermal annealing (Anneal sys, AS-One 150) is performed under nitrogen (N_2) ambient for 120 sec. The turbo pump remained operational throughout the period of growth in order to achieve the lower pressure. The freshly grown pre-annealed samples at room temperature (RT) are labeled as A (for Ge) and C (for Si) and corresponding post-annealed (600 ^{0}C) samples in N_2 ambient pressure are designated as B (for Ge) and D (for Si). The surface morphology and the structures are investigated by AFM and the room temperature optical characterization is made by PL spectrophotometer (Perkin Elmer Ls 55 Luminescence Spectrometer).

3. Results and discussion

The two, the three dimensional AFM images and the height fluctuations of the pre-annealed Ge nanoislands (sample A) are illustrated in Fig. 1a, b and c respectively. The formation of different sizes of islands having estimated height ~10 nm and width ~ 45 nm is clearly evidenced. Fig. 1d, e and f shows the AFM images for the corresponding post-annealed Ge nanoislands (sample B) in which the impact of annealing temperature on growth morphology is clearly reflected. Indeed, the nature of the growth demonstrates the remarkable role played by the thermal treatment. Thermal annealing in fact, make the rearrangement of the inner structure of Ge/Si clusters leading to the formation of varieties of islands with diverse size fluctauations which is exactly evidenced in the micrographs. The nanoislands in the post annealed sample at 600 ^{0}C are gradually grown from pre-annealed one into bigger island structures with average height ~23 nm and width ~125 nm thereby converting the shape of clusters from metastable pyramid to dome-like structure as evidenced from fig.1c and f. This observation is attributed to the mechanism of thermal diffusion and the nucleation of the growth processes.

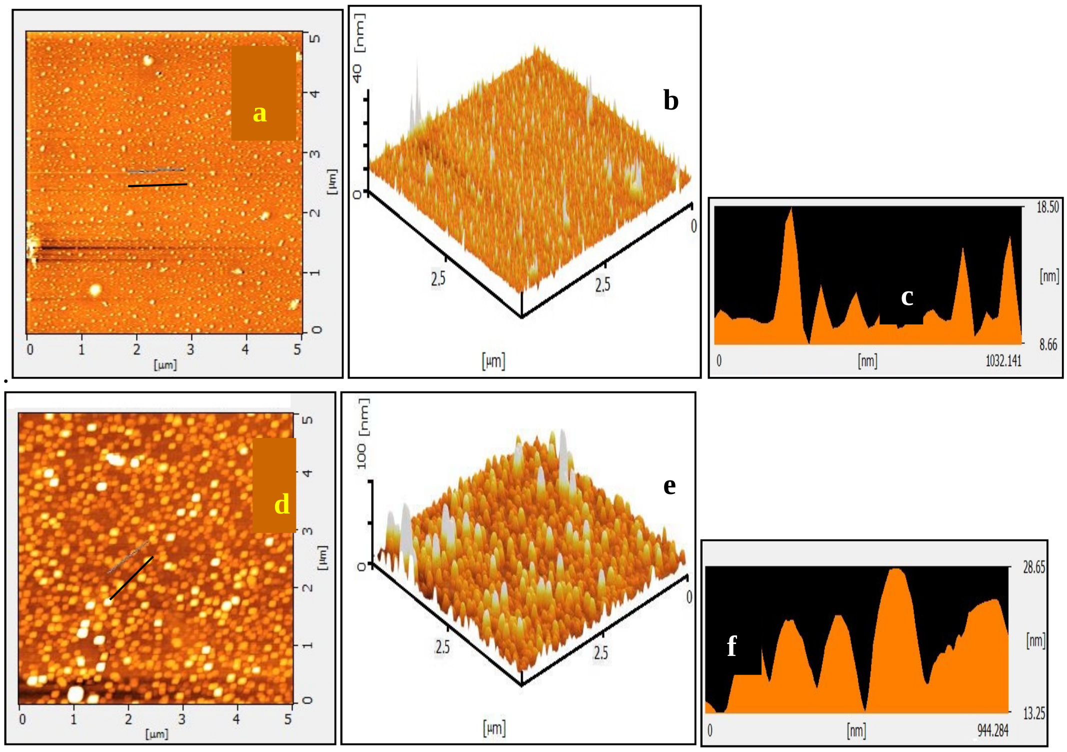

Fig. 1 The AFM images of Ge pre-annealed sample A (upper half) in two dimension (a), three dimension (b), the height fluctuation (c) and the post-annealed sample B (lower half) in two dimension (d), three dimension (e), height fluctuation (f). The line of scan is indicated on two dimensional micrographs.

The cross-section of two, three dimensional AFM images and the height fluctuations of the pre-annealed Si sample (sample C) are shown in Fig. 2a, b and c and for the corresponding post-annealed Si sample (sample D) are depicted in Fig. 2d, e and f respectively. Through annealing process at 600 °C, the Si and nanocrystalline Si (nc-Si) undergoes reaction to finally form the alloy of Si thin film nanostructure with dome shape islands as seen in Fig. 2d, e and f. The variation of dispersive surface energy between them causes inter-diffusion at crossing point and rearrangements of nanoislands. During annealing, the lower value of the interface state energy of bulk Si compare to that of nc-Si favors the Si atoms tend to form interior atoms or shift to the interface. With heat treatment the estimated height of islands found to decrease from ~15 nm to 6 nm and width decrease from ~112 to ~84 nm respectively. The influence of thermal annealing on growth morphology is quite robust.

The fluctuation in the height distribution expressed in terms the root mean square (RMS) roughness is an important factor in deciding the sample quality that eventually controls the optical

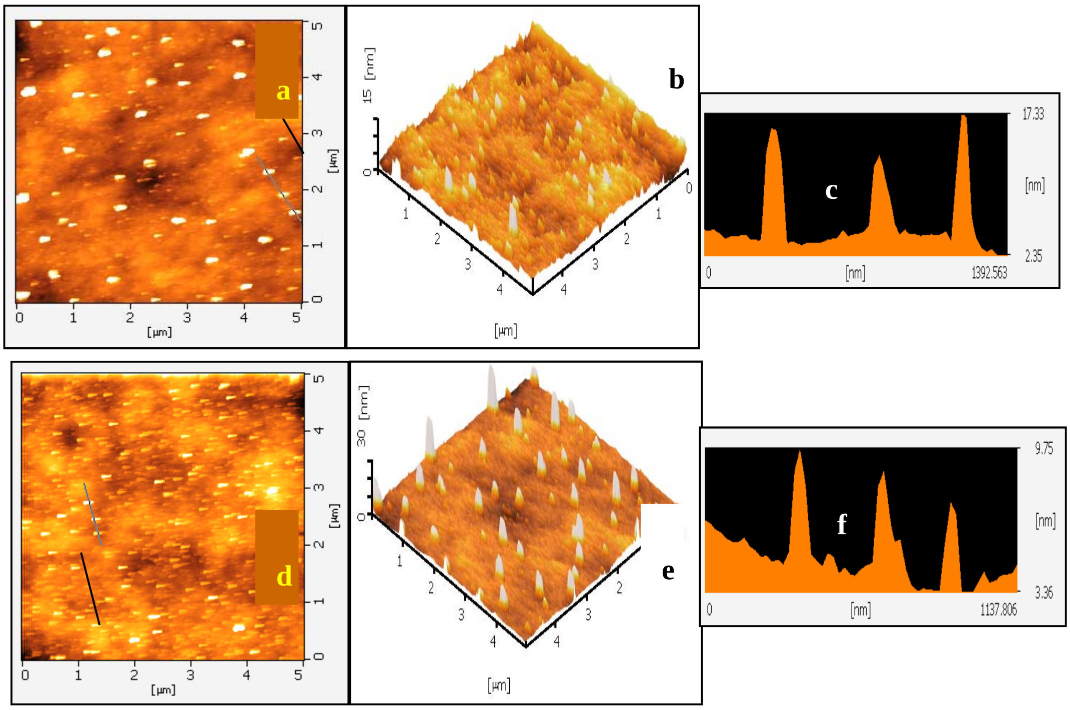

Fig. 2 The AFM images of Si pre-annealed sample C (upper half) in two dimension (a), three dimension (b), the height fluctuation (c) and the post-annealed sample D (lower half) in two dimension (d), three dimension (e), height fluctuation (f). The line of scan is indicated on two dimensional micrographs.

behavior of nanoilands. The variation in RMS roughness for pre-annealed and post-annealed Si and Ge nanoislands along with their height, width, densities and PL peak energies are summarized in table 2. As seen from the table, the annealing temperature dependent RMS roughness shows a rapid increase for Ge islands and steady decrease for Si islands. For Ge samples the majority of the smaller particles coarsen to form larger particles as the temperature is increased that in turn drastically reduced the number density from 12.5 to 2.6. This sharp decrement in the number density can be understood by the kinetics of the growth processes that occurs via thermal diffusion. On the contrary, for Si samples the number density is increased from 1.47 to 1.88. It is worth mentioning that compared to bulk crystalline Si structure, the crystallization of nanoamorphous Si involves several phenomena such as the creation of the crystalline seeds, the influence of the crystal interface, strain and extended defects at the grain boundaries. Beside crystallization of the amorphous Si, annealing process of the sputtered a-Si on nc-Si interface also improve the interface properties substantially. Both the number density and the RMS fluctuations for Si showed much smaller change compared to that of Ge as a function of annealing temperature. However, the red shift of the PL peak energy from 3.22 eV to 3.17 eV with the increase of the annealing temperature confirms the decrease in nanodots size followed by the enhancement of islands density and surface roughness as illustrated in table 2. Furthermore, the value of RMS roughness and number density for Ge quantum structure is found to be more sensitive to the annealing temperature compared to that of Si.

The recorded PL spectra for Ge samples are presented in fig. 3a. The spectra that exhibits three peaks approximately at 2.87, 3.22 eV and 3.96 eV are attributed to the interaction between Ge, GeOx, and the possibility of the formation of core-shell like structure. Annealing the samples at 600 ^{o}C temperature causes the formation of larger dots, the mix state of Ge and the thicker GeOx interface reaction that give rise to the PL peak at around 2.83 eV. The two intense peaks around 3.22 and 3.17 eV are clearly evidenced for samples A, B respectively are attributed to the presence of Ge QDs.

Table 2. The Average height, width, RMS roughness, number density and PL peak position of samples for the pre-annealed and post-annealed samples of Si and Ge.

	Average Height (nm)	Average Width (nm)	RMS Roughness (nm)	Number Density $\times 10^9$ cm^{-2}	PL Peak Position (eV)
Pre-Annealed Si	15	112	1.80	1.47	2.87
Post-Annealed Si	6	84	1.11	1.88	2.53
Pre-Annealed Ge	10	45	1.55	12.51	3.22
Post-Annealed Ge	23	125	8.35	2.62	3.17

The blue shift in the HOMO-LUMO energy gap becomes pronounced upon nanosizing. We assert that the quantum size effect drives the visible PL shift by making the transition from direct band gap to indirect one as confirmed in the literature [20]. The red shift (~ 0.05 eV) of PL peak position after thermal treatment is in closed agreement with the other observations [21- 23].

The room temperature PL spectra of Ge nanocrystalline samples on SiO_2 matrix by ion implantation technique is measured by Mestanza et al where they observed a broad blue violet band at around 3.2 eV (400 nm) that originates from germanium-oxygen-deficient-centers. The presence of a weak peak around 4.0 eV is also reported [21]. The temperature dependent PL peak at 2.05 eV is observed by Sun et al [22]. A shift in the PL peak from 1.18 to 1.05 eV with increasing nanoparticle size from 1.6 to 9.1 nm is reported by Riabinina et al [23]. Three pronounced PL peaks at 2.59 eV, 2.76 eV and 3.12 eV for Ge nanoparticles synthesized by the inert gas condensation (IGC) method are illustrated by Oku et al. The PL peaks are related to luminescence that originates from the Ge/GeOx interface and quantum size effect of Ge clusters. The blue shift of band gap energy is argued due to the formation of the core-shell structure of Ge and Si with oxide layers [19]. Our results on red shift are in consistent with all these observations. The annealing temperature dependent shift in the PL peak position for different sizes of QDs is attributed to quantum confinement effects. The PL intensity that is found to maximum for the sample B with larger size of islands is due to the generation of larger number of photo-carriers that contribute to the emission cross-section significantly. For the pre-annealed sample on the other hand, the appearance of the PL peak at 2.87 eV clearly indicates the formation of mix states and the core-shell like structure in the island. The red shift in the peak position with the annealing process is due to the formation of heavily oxidized nanoparticles as well as bigger core-shell structures. Our results confirm that the formation of core-shell structures, the presence of mix state, the quantum size and surface effects together are responsible for the strong room temperature visible luminescence in Ge QDs.

Fig. 3b shows the room temperature and annealing temperature (600 °C) dependent luminescence from Si nanoislands. It is characterized by a single strong broadband centered at 2.53 eV with two weak satellite peaks. It can be seen from the spectra that pre-annealed film dominates over the post annealed sample. The annealing process allows a redistribution of the emission intensities from the high to the low energy at 2.87 eV. A shift as much as 0.34 eV in the PL peak is observed for the annealed sample. The high luminescence intensity for pre-annealed sample is attributed to the islands recombination, while the low intensity for post-annealed sample at is related to recombination via the a-Si/nc-SiO_2 interface. At room temperatures, the only possible recombination is the spatially indirect transition across the interface for which the electron is located in the amorphous-Si surrounding the nc-Si, while the hole is confined inside the Si nanodot. An increase in the annealing temperature results an increased probability for the electrons to populate the higher energy level inside the dot,

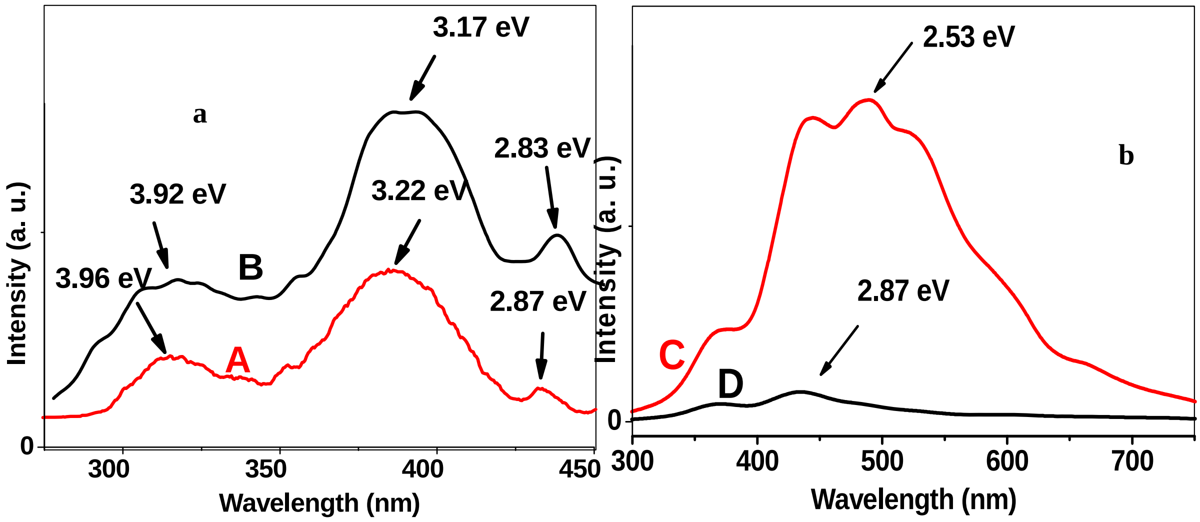

Fig. 3 .The PL spectra for nanoislands of Ge (a) and Si (b).

which opens up the possibility for an alternative recombination channel [13, 24] and thereby causes a blue shift. Moreover, the annealing temperature dependent variation of the PL intensity is significant for Si than Ge.

4. Conclusion

The annealing temperature dependent structural and optical properties of Ge and Si nanoislands fabricated by using RF magnetron sputtering method are investigated. A comparative study between their growth morphology and optical behaviors are studied. The influence of annealing temperature on visible PL and quantum yield are examined. The islands sizes for Ge and Si measured by AFM are found to be ~ 45 nm and ~ 84 nm respectively. The room temperature PL spectra of Si showed a strong luminescence peak at 2.53 eV, which is attributed to the appearance of nanoislands. The Ge nanoislands that exhibited a strong luminescence peak at 3.22 eV is characterized the quantum size and surface effects of the islands. Upon annealing the PL peak for Ge showed a shift ~0.05 eV, where for Si the shift is ~0.34 eV. Size, shape, number density, roughness and PL band are found to be highly sensitive to the heat treatment. The annealing temperature plays a significant role in shifting the PL peak position, broadening the PL band and controlling the overall growth processes. However, the effect of annealing on the growth morphology of Ge nanostructures is appeared to be more pronounced than on Si nanostructure. Therefore, the surface passivation, in addition to the quantum confinement effect, plays an active role in deciding the optical properties and electron correlation of Ge and Si nanostructures. From our investigations, we assert that small-sized Ge and Si quantum dots are promising candidates for visible, tunable and high-quantum-yield light-emitting devices, as predicted by many experimental findings.

Our results on the PL strongly suggest that the photo-generation of carriers occurs in the crystalline silicon core with the band gap modified by the quantum confinement effect while the visible room-temperature photoluminescence comes from the near-surface region of crystallites. This study shows that the radiative recombination in the near-surface region causes the strong visible photoluminescence at room temperature. Our simple results on synthesis and characterizations provide the experimental evidence that the density and roughness of small Ge and Si nanocrystallites can be tuned in the visible range by controlling their sizes useful for optoelectronics as predicted. It is shown that for the oxygen passivated Ge and Si nanoislands a peak in the higher energy region of the luminescence appears in comparison to the bulk Ge and Si. Our observations for the temperature sensitivity of surface morphology showed that the luminescence and the absorption properties are intimately related to the nanometer size of the dots. To understand the detail mechanism of luminescence, it is worth looking at the annealing temperature dependent luminescence efficiency as a function of crystallite size, core-shell like structures and surface passivation. The RF sputtering being an easy, cheap and viable method can be readily used for large scale production of Si and Ge nanoislands of high density suitable for optoelectronic applications.

Acknowledgment

Alireza gratefully acknowledges the technical support from Ibn Sina Institute, Department of Physics, Faculty of Sceince and the international doctoral fellowship (IDF), SPS of Universiti Teknologi Malaysia.

References

[1] L. T. Canham, Silicon Quantum Wire Arrya Fabrication by Electrochemical and Chemical Dissolution of Wafers, Appllied Physics Letter, **57**(10), 1046-1048 (1990).
[2] Y. Kanemitsu, Slow Decay Dynamics of Visible Luminescence in Porous Si: Hopping of Carriers Confined on a Shell Region in Nanometer-sized Si Crystallites, Physical Review B, **48**(16), 12357-12360 (1993).
[3] P. Bettoti, M. Cazzanelli, L. D. Negro, B. Danese, Z. Gaburro, C. J. Oton, G. Vijaya Prakash L Pavesi, Silicon Nanostructures for Photonics, Journal of Physics Condenced Matter, **14**, 8253-8281 (2003).
[4] S. K. Ghoshal, M. R. Sahar and M. S Rohani, Investigation of Optical Effects in Silicon Quantum Dots by Using an Empirical Pseudopotential Method, Journal of Korean Physical Society, **58** (2), 256-264 (2011).
[5] A. Tanakal, Y. Tsuchiya, K. Usami, S. Saito,T. Arai, H. Mizuta and S. Oda, Synthesis of Assembled Nanocrystalline Si Dots Film by the Langmuir-Blodgett Technique, Japanese Journal of Applied Physics, **47** (5), 3731–3734 (2008).
[6] A. R. Samavati, S. K. Ghoshal and Z. Othaman , Influence of annealing on Structural and optical properties of germanium quantum dots, Journal of Ovonic Research, **8**(2), 21-27 (2012).
[7] B. Zhang, S. Shrestha, P. Aliberti, M.A. Green and G. Conibeer, Characterisation of size-controlled and red luminescent Ge nanocrystals in multilayered superlattice structure, Thin Solid Films, **518,** 5483 – 5487 (2010).
[8] S.W. Pan, B. Zhou, S.Y. Chen, C. Li, W. Huang and H. K. Lai,Optical propertiy investigation of SiGe nanocrystal formed by electrochemical anodization, Applied Surface Science **258**, 30– 33 (2011).
[9] W. Xu, H. Tu, D. Liu, R. Teng, Q. Xiao and Q. Chang, Self-assembled SiGe quantum dots embedded in Ge matrix by Si ion implantation and subsequent annealing, Journal of Nanoparticle Research, **14**, 682 (2012).
[10] J. Xu, G. Chen, C. Song, K. Chen, X. Huang and Z. Ma, Formation and properties of high density Si nanodots, Applied Surface Science, **256,** 5691–5694 (2010).
[11] C. Ternon, F. Gourbilleau, R. Rizk and C. Dufour, Si/SiO2 multilayers: synthesis by reactive magnetron sputtering and photoluminescence emission, Physica E, **16,** 517–522 (2003).

[12] S. Huang, Z. Xia, H. Xiao, J. Zheng , Y. Xie and G. Xie, Structure and property of Ge/Si nanomultilayers prepared by magnetron sputtering, Surface & Coating Technology **204**, 558-562 (2009).
[13] K. Y. Kang, S. K. Deng, R. T. Hao, D. C. Li, Characterization and PL Properties of Ge-nduced Crystallization of a-Si Films Deposited by Magnetron Sputtering, Advanced Materials Research, **366,** 99-102 (2012).
[14] M. Zacharias and P. M. Fauchet, Blue luminescence in films containing Ge and GeO2 nanocrystals: The role of defects, Applied Physics Letters **71**, 380-382 (1997).
[15] G. Kartopu, V. A Karavanskii, U. Serincan, R. Turan, R. E. Hummel, Y. Ekinci, A. Gunnæs and T. G. Finstad, Can chemically etched germanium or germanium nanocrystals emit visible photoluminescence?, Physica Status Solidi A **202**, 1472-1476 (2005).
[16] V. L. Thanh, V. Yama, Y. Zhengb and D. Bouchier, Nucleation and growth of self-assembled Ge/Si(001) quantum dots in single and stacked layers, Thin Solid Films, **380**, 2-9 (2000).
[17] A. F. Khan, M. Mehmood, A. M. Rana and T. Muhammad, Effect of annealing on structural, optical and electrical properties of nanostructured Ge thin films, Applied Surface Science, **256**, 2031-2037 (2010).
[18] W. Zhao, O. Schoenfeld, Y. Aoyagi, T. Sugano, Violet luminescence from anodized microcrystalline silicon, Applied Physics Letter, **65**, 1290–1292 (1994).
[19] Oku T, Nakayama T, Kuno M, Nozue Y, Wallenberg L R, Niihara K and Suganuma K , Formation and photoluminescence of Ge and Si nanoparticles encapsulated in oxide layers, Materials Science and Engendering B, **74,** 242 (2000).
[20] T. Takagahara and K. Takeda, Theory of the quantum confinement effect on excitons in quantum dots of indirect-gap materials, Physical Review B, **46**,15578-15581 (1992).
[21] S. N. M. Mestanza, E. Rodriguez and N. C. Frateschi, The effect of Ge implantation dose on the optical properties of Ge nanocrystals in SiO2, Nanotechnology, **17**, 4548-4553 (2006).
[22] K. W. Sun, S. H. Sue and C. W. Liu, Visible photoluminescence from Ge quantum dots, Physica E, **28**, 525-530 (2005).
[23] D. Riabinina, C. Durand and M. Chaker, Anovel approach tothesynthesis of photoluminescent germanium nanoparticles by reactive laser ablation, Nanotechnology, **17**, 2152-2155 (2006).
[24] C. Ternon, F. Gourbilleau, X.Portier, P.V oivenel, C. Dufour, An original approach for the fabrication of SiySiO multilayers using reactive magnetron sputtering, Thin Solid Films, **419,** 5–10 (2002).